






StainDiff: Transfer Stain Styles of Histology Images with Denoising Diffusion Probabilistic Models and Self-ensemble

Yiqing Shen¹  and Jing Ke^{2,3}  

¹ Department of Computer Science, Johns Hopkins University, Baltimore, USA
yshen92@jhu.edu

² School of Electronic Information and Electrical Engineering, Shanghai Jiao Tong University, Shanghai, China
kejing@sjtu.edu.cn

³ School of Computer Science and Engineering, University of New South Wales, Kensington, Australia

Abstract. The commonly presented histology stain variation may moderately obstruct the diagnosis of human experts, but can considerably downgrade the reliability of deep learning models in various diagnostic tasks. Many stain style transfer methods have been proposed to eliminate the variance of stain styles across different medical institutions or even different batches. However, existing solutions are confined to Generative Adversarial Networks (GANs), AutoEncoders (AEs), or their variants, and often fell into the shortcomings of mode collapses or posterior mismatching issues. In this paper, we make the first attempt at a Diffusion Probabilistic Model to cope with the indispensable stain style transfer in histology image context, called **StainDiff**. Specifically, our diffusion framework enables learning from unpaired images by proposing a novel cycle-consistent constraint, whereas existing diffusion models are restricted to image generation or fully supervised pixel-to-pixel translation. Moreover, given the stochastic nature of **StainDiff** that multiple transferred results can be generated from one input histology image, we further boost and stabilize the performance by the proposal of a novel self-ensemble scheme. Our model can avoid the challenging issues in mainstream networks, such as the mode collapses in GANs or alignment between posterior distributions in AEs. In conclusion, **StainDiff** suffices to increase the stain style transfer quality, where the training is straightforward and the model is simplified for real-world clinical deployment.

Keywords: Diffusion Probabilistic Model · Histology Stain Transfer

1 Introduction

Staining is a vital process in preparing tissue samples for histology studies. Specifically, with dyes such as Hematoxylin and Eosin, transparent tissue elements can be transformed into distinguishable features [1]. However, stain styles can vary significantly across different pathology labs or institutions. These variations can be due to the difference in staining materials, protocols, or processes among different pathologists or digital scanners [16, 23]. Yet, the stain variations can cause inconsistencies between human domain experts [11]; and also hinder the performance of computer-aided diagnostic (CAD) systems [5, 7]. Moreover, experiments have shown that stain variations can lead to a significant decrease in the accuracy and reproducibility of deep learning algorithms in histology analysis. Consequently, it is crucial to minimize staining variations to ensure reliable, consistent, and accurate CAD systems.

To address the issue of stain variations between different domains, stain style transfer has been proposed. While the conventional color matching [22] and stain separation methods [19] used to be popular; learning-based approaches have become increasingly dominant, because they eliminate the need for challenging manual selection of the template images. For example, Stain-to-Stain Translation (STST) [25] approaches stain style transfer within a fully supervised ‘pix2pix’ framework [12]. Another approach, called StainGAN [26], improves on STST by tailoring a CycleGAN [34] to get rid of the dependence on learning from paired histology images and enable an unsupervised learning manner. These methods have shown promising results in reducing staining variations.

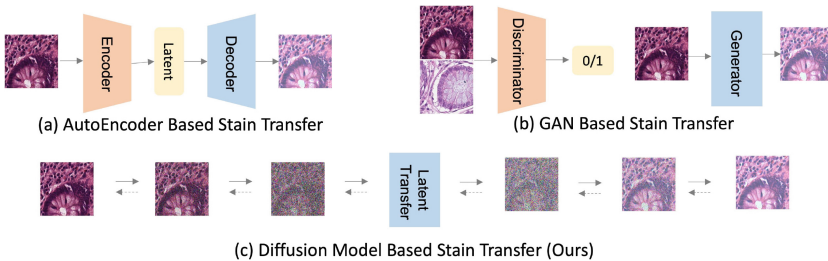


Fig. 1. Different generative model based stain style transfer solutions. (a) AutoEncoder (AE). (b) GAN. (c) Our proposed diffusion based **StainDiff**.

Existing learning-based methods for stain style transfer are primarily confined to Generative Adversarial Networks (GANs) [6] and AutoEncoder (AE) [2], as depicted in Fig. 1(a) and (b) respectively. However, GAN approaches and AE suffer from the training of extra discriminators and challenging alignment of the posterior distributions, respectively [27]. In contrast, diffusion models, such as the prevalent denoising diffusion probabilistic model (DDPM) [9], have emerged as an alternative approach that can achieve competitive performance in various

image-related tasks, such as image generation, inpainting, super-resolution, and *etc* [3]. Importantly, diffusion models offer several advantages over GANs and AEs, including tractable probabilistic parameterization, stable training procedures, and theoretical guarantees [3]. Additionally, they can avoid some of the challenges encountered by GANs and AEs, such as the alignment of posterior distributions or training extra discriminators, leading to a simpler model and training process. However, the applicability of diffusion models to histology stain style transfer remains unexplored. While the current diffusion models focus on image synthesis [9] or supervised image-to-image transaction [24], they are not applicable to our circumstance, as obtaining paired histology slides with different stain styles is not feasible in real clinical practice [27]. Therefore, we design an innovative cycle-consistent diffusion model that allows the transfer of representations between latent spaces at different time steps with the same morphological structure preserved in an unsupervised manner, as shown in Fig. 1(c).

The major contributions are three-fold, summarized as follows. (1) We propose **StainDiff**, which is the first attempt at a pure denoising diffusion probabilistic model for stain transfer. More innovatively, unlike existing diffusion models, **StainDiff** is capable of learning from unpaired histology images, making it a more flexible and practical solution. The model is superior to GAN-based methods as the training of additional discriminators is free, and also spares for the difficulty in the alignment of posterior probabilities in AE-based approaches. (2) We also propose a self-ensemble scheme to further improve and stabilize the style transfer performance in **StainDiff**. This scheme utilizes the stochastic property of the diffusion model to generate multiple slightly different outputs from one input at the inference stage. (3) A broad range of histology tasks, such as stain normalization between multiple clients, can be conveniently achieved with minor adjustment to the loss in **StainDiff**.

2 Methods

Overview. The goal of this work is to design a diffusion model [9] to transfer the stain style between two domains, *i.e.*, $\mathcal{X}^A, \mathcal{X}^B$. However, the traditional training paradigm of conditional DDPMs with paired images $(\mathbf{x}_0^A, \mathbf{x}_0^B) \in \mathcal{X}^A \times \mathcal{X}^B$ is not feasible, as they are unavailable in the context of histology. To overcome this limitation, we design an innovative diffusion framework for stain style transfer, named **StainDiff**, which leverages the success of CycleGAN [34] and StyleGAN [26] and thus can be trained in an unsupervised manner with a novel cycle-consistency constraint. Specifically, **StainDiff** comprises two forward processes that perturb the histology image of two stain style domains to noise respectively, and two corresponding reverse processes that attempt to reconstruct noise back to original images from the perturbed ones. The overall training process is depicted in Fig. 2.

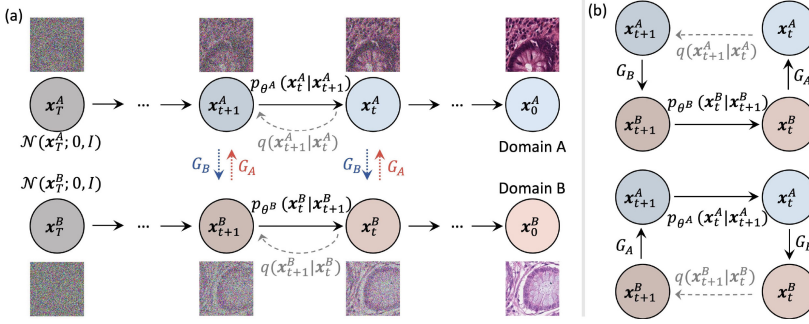


Fig. 2. (a) The directed graphical model for the training process of the proposed **StainDiff**. It comprises two diffusion paths, that each learns the histology image generation with respect to one stain style domain. The interplay between two domains is learned by a paired auxiliary transform network G_A and G_B through a cycle-consistency constraint. (b) We specify the consistency cycles to impose the regularization.

Forward Process. Parameterized by the Markov chain, the forward process in **StainDiff** follows the vanilla DDPM by perturbing the histology images gradually with Gaussian noise, until all structures and morphological context information are lost. Formally, given a histology image \mathbf{x}_0^A with respect to the stain style domain A , a transition kernel q progressively generates a sequence of T latent variables $\mathbf{x}_1^A, \mathbf{x}_2^A, \dots, \mathbf{x}_T^A$ thorough the following equation:

$$q(\mathbf{x}_t^A | \mathbf{x}_{t-1}^A) = \mathcal{N}(\mathbf{x}_t^A; \sqrt{1 - \beta_t} \mathbf{x}_{t-1}^A, \beta_t \mathbf{I}), \quad (1)$$

where $\mathcal{N}(\cdot)$ denotes the Gaussian distribution, \mathbf{I} is the identity matrix. The hyper-parameters β_t s follow a linear rule as defined in DDPM [9] to guarantee $q(\mathbf{x}_T^A) = \int q(\mathbf{x}_T^A | \mathbf{x}_0^A) q(\mathbf{x}_0^A) d\mathbf{x}_0^A \approx \mathcal{N}(\mathbf{x}_T^A; \mathbf{0}, \mathbf{I})$. Identically, we can progress the latent variables $\mathbf{x}_1^B, \mathbf{x}_2^B, \dots, \mathbf{x}_T^B$ for the histology image \mathbf{x}_0^B from the stain style domain B in the same fashion as Eq. (1).

Reverse Process and Cycle-Consistency Constraint. The reverse process in **StainDiff** optimizes two conditional diffusion models, namely $p(\mathbf{x}^A | \mathbf{x}^B)$ and $p(\mathbf{x}^B | \mathbf{x}^A)$, to transfer the stain style between two domains A and B . Concretely, two learnable transition kernels $p_{\theta^A}(\mathbf{x}_t^A | \mathbf{x}_{t+1}^B)$ and $p_{\theta^B}(\mathbf{x}_t^B | \mathbf{x}_{t+1}^A)$ learns to reverse the Eq. (1) and generate images characterized by stain style A and B respectively, by gradually removing the noise initialized from Gaussian prior. To ensure conservative outputs [24], L1-norm denoising objective \mathcal{L}_d [4] is leveraged to train the denoising networks in the transition kernels. Due to the absence of pixel-to-pixel paired histology of both stain styles, it is infeasible to learn the interplay between them in a supervised manner as in most previous works. Consequently, a pair of auxiliary transform networks $G_A : \mathbf{x}_t^B \mapsto \mathbf{x}_t^A$ and $G_B : \mathbf{x}_t^A \mapsto \mathbf{x}_t^B$ are designed to learn the transfer between the latent variables across the two

domains in an unsupervised fashion, using a novel cycle-consistency constraint. Formally, this constraint ensures that two cycles as depicted in Fig. 2(b), derive an identity mapping, *i.e.*,

$$\begin{cases} \mathbf{x}_{t+1}^A &= q \circ G_A \circ p_{\theta^B} \circ G_B(\mathbf{x}_{t+1}^A), \\ \mathbf{x}_{t+1}^B &= q \circ G_B \circ p_{\theta^A} \circ G_A(\mathbf{x}_{t+1}^B), \end{cases} \quad (2)$$

where \circ denotes the composition of operations. It follows the cycle-consistency constraint formulated by

$$\mathcal{L}_c = \mathbb{E}_{t, \mathbf{x}_0^A} \|\tilde{\mathbf{x}}_{t+1}^A - \mathbf{x}_{t+1}^A\| + \mathbb{E}_{t, \mathbf{x}_0^B} \|\tilde{\mathbf{x}}_{t+1}^B - \mathbf{x}_{t+1}^B\|, \quad (3)$$

where $\tilde{\mathbf{x}}_{t+1}^A$ and $\tilde{\mathbf{x}}_{t+1}^B$ are defined by Eq. (2); \mathbb{E} denotes the expectation; $\|\cdot\|$ is the L1-norm. Finally, the overall loss function is $\mathcal{L} = \mathcal{L}_d + \gamma \mathcal{L}_c$, balanced by the coefficient γ .

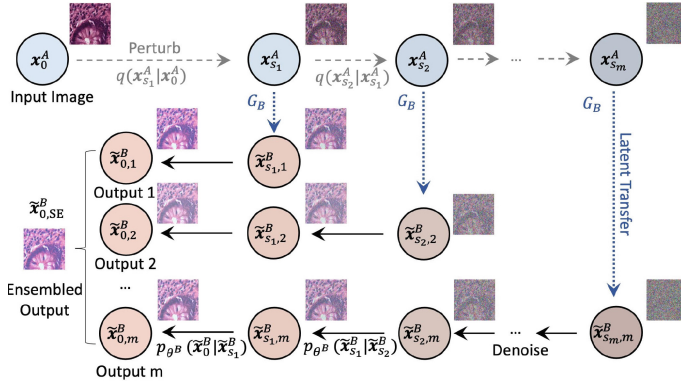


Fig. 3. The directed graphical model for the inference stage with self-ensemble scheme of the StainDiff.

Inference Process and Self-ensemble. We describe the inference stage of StainDiff by transferring the histology images from stain style A to B ; while the inverse, namely from B to A , is similar. Given a histology image input \mathbf{x}_0^A characterized by stain style A , we begin by perturbing it s steps with Eq. (1) to derive \mathbf{x}_s^A . Choosing the optimal value for s is important, as a large s (*e.g.*, $s = T$) leads to the loss of the contextual and structural information; while a small valued s (*e.g.*, $s = 1$) fails to inject sufficient noise for StainDiff to transfer style. An ideal range for s is a small subset from $[1, T]$ that is centered by $\frac{1}{2}T$. Consequently, in this work, we fix s in the range of $[S_1, S_2]$ with $S_1 = \frac{2}{5}T$ and $S_2 = \frac{3}{5}T$. Afterwards, the latent variable \mathbf{x}_s^A is transferred into the corresponding latent space with respect to stain style B with auxiliary transform network G_B , which gives us $\tilde{\mathbf{x}}_s^B = G_B(\mathbf{x}_s^A)$. Next, we use the p -sample [9] iteratively to denoise the $\tilde{\mathbf{x}}_s^B$ and obtain the transferred image $\tilde{\mathbf{x}}_0^B$. As the sampling is a stochastic

process, different values of s result in a slight difference in the transferred output. We exploit this property and propose a novel self-ensemble method that can implicitly generate an ensemble of transferred output without the need to train extra models. Specifically, we repeat the above process for m times with different s i.e., $s_1, \dots, s_m \in [S_1, S_2]$, and come to m outputs $\tilde{\mathbf{x}}_{0,i}^B$ with $i = 1, \dots, m$. The self-ensemble transferred output is then given by $\tilde{\mathbf{x}}_{0,SE}^B = \sum_{i=1}^m \tilde{\mathbf{x}}_{0,i}^B$. The graphical model for the inference process and the proposed self-ensemble scheme are summarized in Fig. 3.

Extension to Stain Normalization. The stain transfer primarily addresses the domain gap between two stain styles, which is mathematically formulated as a one-to-one mapping. Meanwhile, in some clinical settings, multiple institutions or hospitals are involved, where stain normalization is usually employed for multiple stain styles to one style alignment. The proposed symmetric **StainDiff** structure can be easily adapted to support stain normalization, with minimal change to the loss in Eq. (3). Concretely, we assume that domain A comprises multiple stain styles and domain B identifies the targeted stain style. By discarding the second term in Eq. (3), **StainDiff** becomes asymmetric and focuses specifically on the transfer from domain A to B . This modification allows us to use **StainDiff** for stain normalization without any other adjustments to the inference process.

3 Experiments

Datasets. Evaluations of **StainDiff** are conducted on two datasets. (1) Dataset-A: *MITOS-ATYPIA 14 Challenge*¹. This dataset aims to measure the style transfer performance on 284 histology frames. Each slide is digitized by two different scanners, resulting in stain style variations. For a fair comparison, we follow the settings in previous work [26] by using 10,000 unpaired patches randomly cropped from the first 184 slides of both scanners as the training set. Meanwhile, 500 paired patches are generated from the remaining 100 slides as the test set, where we use Pearson correlation coefficient (PC), Structural Similarity index (SSIM) [31] and Feature Similarity Index for Image Quality Assessment (FSIM) [33] as the evaluation metrics. (2) Dataset-B: *The Cancer Genome Atlas (TCGA)*. This dataset evaluates the performance of stain normalization quantified by the downstream nine-category tissue structure classification accuracy [27]. Domain A contains histology of multiple stain styles, which are collected from 186 WSIs from TCGA-COAD and NCT-CRC-HE-100K [14]; and domain B is the target style, curated from 25 WSIs in CRC-VAL-HE-7K [14].

Implementations. All experiments are implemented in Python 3.8.13 with Pytorch 1.12.1 on two NVIDIA GeForce RTX 3090 GPU cards with 24GiB of

¹ <https://mitos-atypia-14.grand-challenge.org>.

Table 1. Comparison of stain style transfer performance on Dataset-A. To show the statistical significance, the p -values in terms of SSIM and FSIM are computed with respect to **StainDiff** (full setting). The ‘w/o SE’ denotes the exclusion of the self-ensemble scheme from the inference stage.

Method	PC (\uparrow)	SSIM (\uparrow)	FSIM (\uparrow)	p_{SSIM}	p_{FSIM}
Reinhard [22]	0.509 \pm 0.091	0.587 \pm 0.041	0.668 \pm 0.032	1.0×10^{-5}	2.0×10^{-5}
Macenko [19]	0.507 \pm 0.108	0.554 \pm 0.084	0.675 \pm 0.024	3.2×10^{-4}	1.1×10^{-4}
Khan [17]	0.563 \pm 0.053	0.643 \pm 0.049	0.702 \pm 0.032	1.4×10^{-5}	5.7×10^{-5}
Vahadane [30]	0.561 \pm 0.058	0.639 \pm 0.063	0.710 \pm 0.031	8.8×10^{-5}	3.5×10^{-4}
StaNoSa [13]	0.552 \pm 0.081	0.647 \pm 0.070	0.692 \pm 0.044	4.1×10^{-4}	1.2×10^{-4}
StainGAN [26]	0.572 \pm 0.049	0.692 \pm 0.072	0.723 \pm 0.014	3.2×10^{-3}	1.4×10^{-4}
Harshal [21]	0.552 \pm 0.047	0.685 \pm 0.033	0.705 \pm 0.026	6.2×10^{-4}	2.7×10^{-4}
MWB [20]	0.543 \pm 0.107	0.690 \pm 0.052	0.718 \pm 0.032	1.2×10^{-3}	2.0×10^{-3}
CL-StainGAN [15]	0.585 \pm 0.039	0.701 \pm 0.034	0.734 \pm 0.022	2.4×10^{-3}	4.0×10^{-3}
StainDiff (w/o SE)	0.590\pm0.019	0.709\pm0.010	0.742\pm0.007	2.3×10^{-3}	3.0×10^{-3}
StainDiff (Full)	0.599\pm0.025	0.721\pm0.017	0.753\pm0.010	—	—

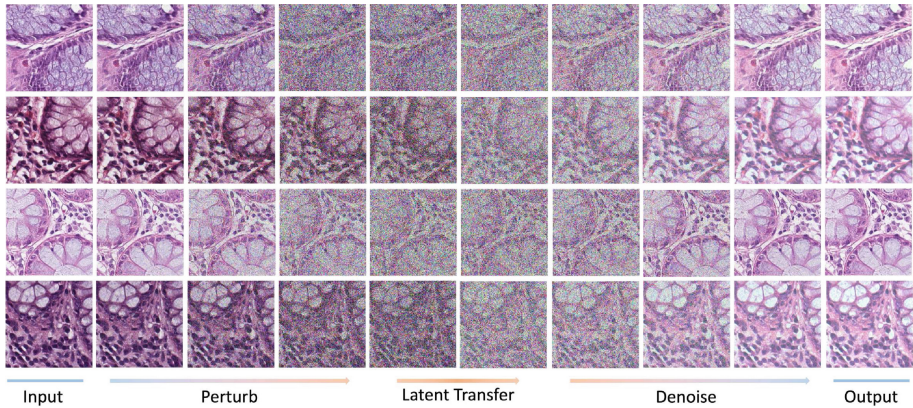


Fig. 4. Visualization of the progressive stain style transfer process in **StainDiff**.

memory each in parallel. We leverage the Adam optimizer with a learning rate of 2×10^{-4} , and a batch size of 4. The learning scheme follows previous work [18], where the training process continues for 100 epochs if the overall loss did not decrease to the average loss of the previous 20 epochs. For **StainDiff**, we set the diffusion time $T = 1000$, the balancing coefficient $\gamma = 1$, and ensemble number $m = 10$. All experiments are repeated for 7 runs with different fixed random seeds *i.e.*, $\{0, 1, 2, 3, 4, 5, 6\}$; and metrics are reported in the form of mean \pm standard deviation.

Table 2. Comparison of the downstream classification task w.r.t. accuracy (%). ‘w/o SE’ denotes excluding the self-ensemble scheme from the inference stage.

Method	ResNet-18	ResNet-50	DenseNet-121	DenseNet-169	EfficientNet
Reinhard [22]	92.10±0.58	93.11±0.39	92.04±0.74	91.17±0.33	92.48±0.99
Macenko [19]	90.35±1.20	90.55±1.43	90.47±1.53	89.99±1.04	91.24±0.85
Khan [17]	91.89±0.83	92.04±0.63	92.22±0.75	92.54±0.55	93.04±0.81
Vahadane [30]	92.87±0.35	93.01±0.42	92.94±0.50	93.31±0.52	93.51±0.39
StaNNoSa [13]	93.25±0.78	93.88±0.21	94.41±0.78	94.60±0.99	94.48±0.53
StainGAN [26]	93.98±0.28	94.21±0.47	93.89±0.21	93.99±0.36	94.52±0.32
Harshal [21]	94.17±0.72	94.58±0.54	93.85±0.80	93.96±0.65	95.03±0.99
MWB [20]	94.56±0.93	95.15±0.79	94.14±0.68	94.32±0.39	95.25±0.55
CL-StainGAN [15]	96.22±0.73	96.89±0.38	95.98±0.58	96.04±0.29	96.49±0.57
StainDiff (w/o SE)	96.79±0.23	97.54±0.47	96.01±0.30	97.00±0.21	97.32±0.35
StainDiff (Full)	97.48±0.10	98.12±0.09	96.98±0.07	97.93±0.11	98.42±0.08

Evaluations on Style Transfer. The superiority of our diffusion model to GANs and AEs in histology stain style transfer is quantitatively reflected in Table 1. Specifically, on Dataset-A, **StainDiff** can surpass its counterparts with a large margin regarding all three metrics. Notably, **StainDiff** achieves the highest SSIM of 0.717 and FSIM of 0.753, which improves the state-of-the-art CL-StainGAN [15] by 0.016 and 0.019 respectively, without reliance on time-costly self-supervised pre-training. Moreover, the statistical significance of our performance boost is validated by the p -values that are consistently smaller than 0.005, as computed from the Wilcoxon signed-rank test. The progressive transfer process of **StainDiff** over time is visualized in Fig. 4.

Evaluations on Stain Normalization. Table 2 presents the comparison results of the downstream classification task, where the histology images in Dataset-B are normalized using different methods. The table clearly shows that **StainDiff** outperforms all the other methods and achieves the highest test accuracy across all five network architectures [8, 10, 29]. Consequently, it yields the superiority of **StainDiff** in terms of stain normalization is model-agnostic.

Ablation Study. Table 1 and 2 show that incorporating a self-ensemble scheme can both boost the performance of **StainDiff**, and bring down the variations, demonstrating its effectiveness in stabilizing the stain transfer and normalization. To further investigate the effect of ensemble number m , we conduct ablation on Dataset-A. Experimentally, the FSIM when $m = 1, 5, 10, 15, 20, 50$ are 0.742, 0.749, 0.753, 0.756, 0.759, 0.759 respectively. While a slight performance gain can be achieved with higher m values than 10, the ensemble becomes more time-consuming, as the cost time is linear to m . It implies an optimal m should be selected as a trade-off between the performance and computational time, such as 10 in this work.

4 Conclusion

In this paper, we propose **StainDiff**, a denoising diffusion model for histological stain style transfer, hence a model can get rid of the challenging issues in mainstream networks, such as the mode collapses in GANs or alignment between posterior distributions in AEs. Innovatively, by imposing a cycle-consistent constraint imposed on latent spaces, **StainDiff** enables learning from unpaired histology images, making it widely applicable to real clinical settings. One future work will explore efficient sampling diffusion models, *e.g.*, DDIM [28], to address the long sampling time issue as inherited from DDPM. Another direction is to investigate other formulations of the diffusion model in the context of stain transfer, such as score-based or score-SDE diffusion models [32]. These extensions will fully expand the scope of our work, hence further advancing towards a comprehensive solution of stain style transfer in histology images.

Acknowledgement. J. Ke was supported by National Natural Science Foundation of China (Grant No. 62102247) and Natural Science Foundation of Shanghai (No. 23ZR1430700).

References

1. Anderson, J.: An introduction to routine and special staining (2011). Accessed 18 Aug 2014
2. Bengio, Y., et al.: Greedy layer-wise training of deep networks. *Adv. Neural Inf. Process. Syst.* **19**, 1–8 (2006)
3. Cao, H., et al.: A survey on generative diffusion model. *arXiv preprint arXiv:2209.02646* (2022)
4. Chen, N., et al.: Wavegrad: estimating gradients for waveform generation. In: *International Conference on Learning Representations* (2020)
5. Ciompi, F., et al.: The importance of stain normalization in colorectal tissue classification with convolutional networks. In: *2017 IEEE 14th International Symposium on Biomedical Imaging (ISBI 2017)*, pp. 160–163. *IEEE* (2017)
6. Goodfellow, I., et al.: Generative adversarial networks. *Commun. ACM* **63**(11), 139–144 (2020)
7. Gupta, V., Singh, A., Sharma, K., Bhavsar, A.: Automated classification for breast cancer histopathology images: is stain normalization important? In: Cardoso, M.J., et al. (eds.) *CARE/CLIP -2017. LNCS*, vol. 10550, pp. 160–169. Springer, Cham (2017). https://doi.org/10.1007/978-3-319-67543-5_16
8. He, K., et al.: Deep residual learning for image recognition. In: *Proceedings of the IEEE Conference on Computer Vision and Pattern Recognition*, pp. 770–778 (2016)
9. Ho, J., Jain, A., Abbeel, P.: Denoising diffusion probabilistic models. *Adv. Neural Inf. Process. Syst.* **33**, 6840–6851 (2020)
10. Huang, G., et al.: Densely connected convolutional networks. In: *Proceedings of CVPR*, pp. 4700–4708 (2017)
11. Ismail, S.M., et al.: Observer variation in histopathological diagnosis and grading of cervical intraepithelial neoplasia. *Brit. Med. J.* **298**(6675), 707–710 (1989)

12. Isola, P., et al.: Image-to-image translation with conditional adversarial networks. In: Proceedings of the IEEE Conference on Computer Vision and Pattern Recognition, pp. 1125–1134 (2017)
13. Janowczyk, A., et al.: Stain normalization using sparse autoencoders (stanosa): application to digital pathology. *Comput. Med. Imaging Graph.* **57**, 50–61 (2017)
14. Kather, J.N., Halama, N., Marx, A.: 100,000 histological images of human colorectal cancer and healthy tissue. Zenodo (2018)
15. Ke, J., Shen, Y., Liang, X., Shen, D.: Contrastive learning based stain normalization across multiple tumor in histopathology. In: de Bruijne, M., et al. (eds.) MICCAI 2021. LNCS, vol. 12908, pp. 571–580. Springer, Cham (2021). https://doi.org/10.1007/978-3-030-87237-3_55
16. Ke, J., et al.: Multiple-datasets and multiple-label based color normalization in histopathology with cgan. In: Medical Imaging 2021: Digital Pathology, vol. 11603, pp. 263–268. SPIE (2021)
17. Khan, A.M., et al.: A nonlinear mapping approach to stain normalization in digital histopathology images using image-specific color deconvolution. *IEEE Trans. Biomed. Eng.* **61**(6), 1729–1738 (2014)
18. Lyu, Q., Wang, G.: Conversion between ct and mri images using diffusion and score-matching models. arXiv preprint [arXiv:2209.12104](https://arxiv.org/abs/2209.12104) (2022)
19. Macenko, M., et al.: A method for normalizing histology slides for quantitative analysis. In: 2009 IEEE International Symposium on Biomedical Imaging: From Nano to Macro, pp. 1107–1110. IEEE (2009)
20. Nadeem, S., Hollmann, T., Tannenbaum, A.: Multimarginal wasserstein barycenter for stain normalization and augmentation. In: Martel, A.L., et al. (eds.) MICCAI 2020. LNCS, vol. 12265, pp. 362–371. Springer, Cham (2020). https://doi.org/10.1007/978-3-030-59722-1_35
21. Nishar, H., Chavanke, N., Singhal, N.: Histopathological stain transfer using style transfer network with adversarial loss. In: Martel, A.L., et al. (eds.) MICCAI 2020. LNCS, vol. 12265, pp. 330–340. Springer, Cham (2020). https://doi.org/10.1007/978-3-030-59722-1_32
22. Reinhard, E., et al.: Color transfer between images. *IEEE Comput. Graph. Appl.* **21**(5), 34–41 (2001)
23. Rubin, R., Strayer, D.S., Rubin, E., et al.: Rubin’s pathology: clinicopathologic foundations of medicine. Lippincott Williams & Wilkins (2008)
24. Saharia, C., et al.: Palette: image-to-image diffusion models. In: ACM SIGGRAPH 2022 Conference Proceedings, pp. 1–10 (2022)
25. Salehi, P., Chalechale, A.: Pix2pix-based stain-to-stain translation: a solution for robust stain normalization in histopathology images analysis. In: 2020 International Conference on Machine Vision and Image Processing (MVIP), pp. 1–7. IEEE (2020)
26. Shaban, M.T., et al.: Staingan: stain style transfer for digital histological images. In: 2019 IEEE 16th International Symposium on Biomedical Imaging (ISBI 2019), pp. 953–956. IEEE (2019)
27. Shen, Y., et al.: A federated learning system for histopathology image analysis with an orchestral stain-normalization gan. *IEEE Trans. Med. Imaging* **42**, 1969–1981 (2022)
28. Song, J., et al.: Denoising diffusion implicit models. arXiv preprint [arXiv:2010.02502](https://arxiv.org/abs/2010.02502) (2020)
29. Tan, M., Le, Q.: Efficientnet: rethinking model scaling for convolutional neural networks. In: International Conference on Machine Learning, pp. 6105–6114. PMLR (2019)

30. Vahadane, A., et al.: Structure-preserving color normalization and sparse stain separation for histological images. *IEEE Trans. Med. Imaging* **35**(8), 1962–1971 (2016)
31. Wang, Z., et al.: Image quality assessment: from error visibility to structural similarity. *IEEE Trans. Image Process.* **13**(4), 600–612 (2004)
32. Yang, L., et al.: Diffusion models: a comprehensive survey of methods and applications. *arXiv preprint [arXiv:2209.00796](https://arxiv.org/abs/2209.00796)* (2022)
33. Zhang, L., et al.: Fsim: a feature similarity index for image quality assessment. *IEEE Trans. Image Process.* **20**(8), 2378–2386 (2011)
34. Zhu, J.Y., et al.: Unpaired image-to-image translation using cycle-consistent adversarial networks. In: *Proceedings of the IEEE International Conference on Computer Vision*, pp. 2223–2232 (2017)